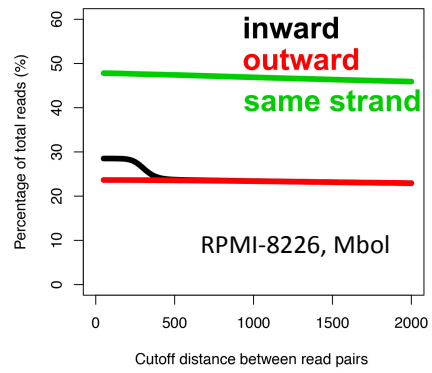
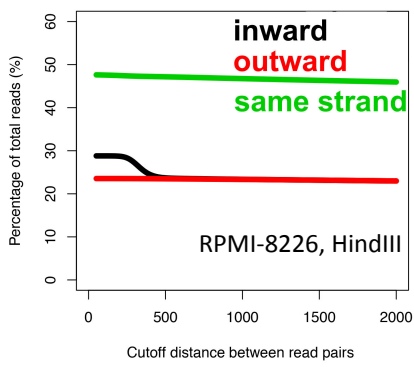
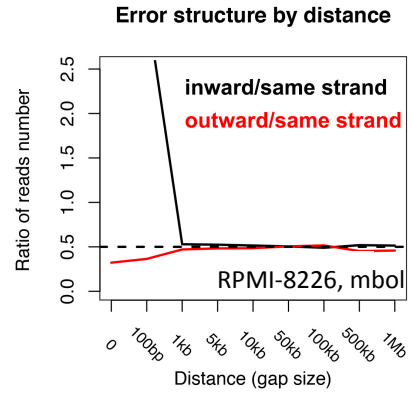
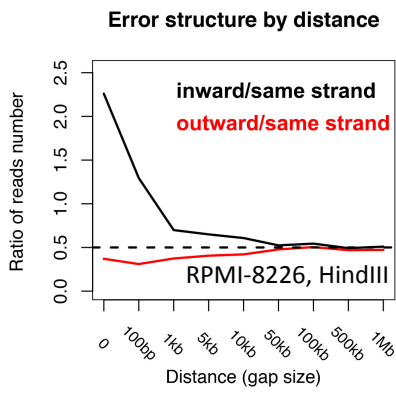


Supplementary Figure 1. Karyotypes of RPMI-8226 and U266 cells. (a–b) Karyotypes of RPMI-8226 cell line. (c–d) Karyotypes of U266 cell line. (e) Estimated CNVs in RPMI-8226 and U266 using WGS data.

a

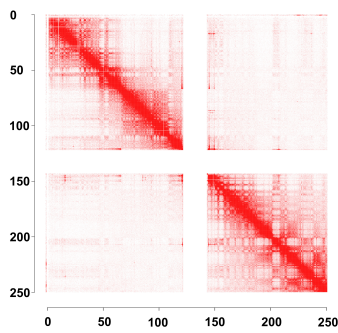


b

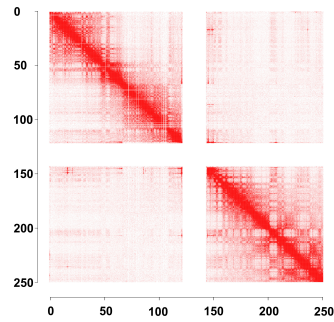


c

RPMI-8226, chr 1, HindIII

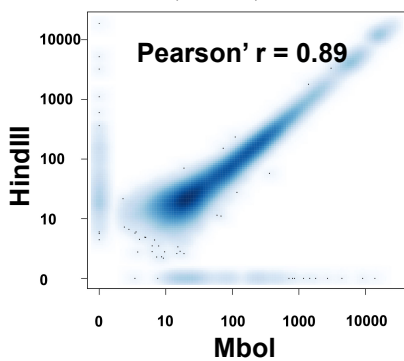


RPMI-8226, chr 1, Mbol

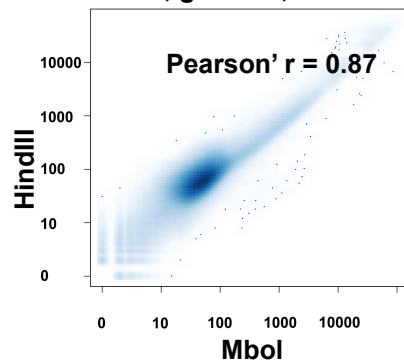


d

RPMI-8226, chr 1, Interactions

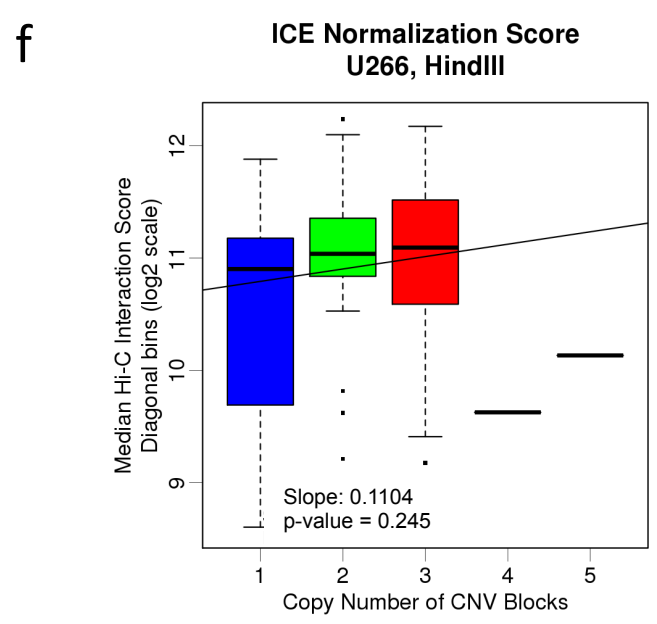
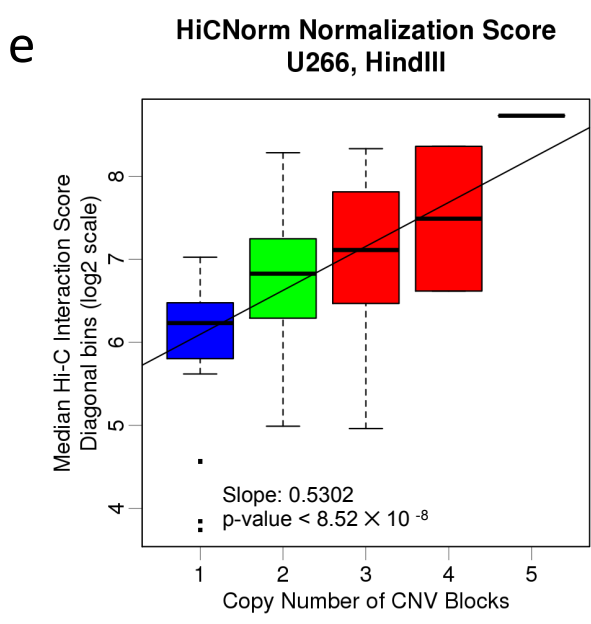
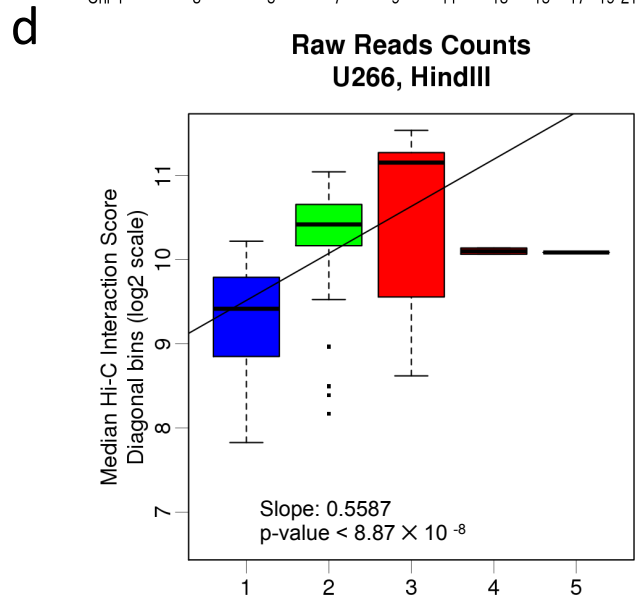
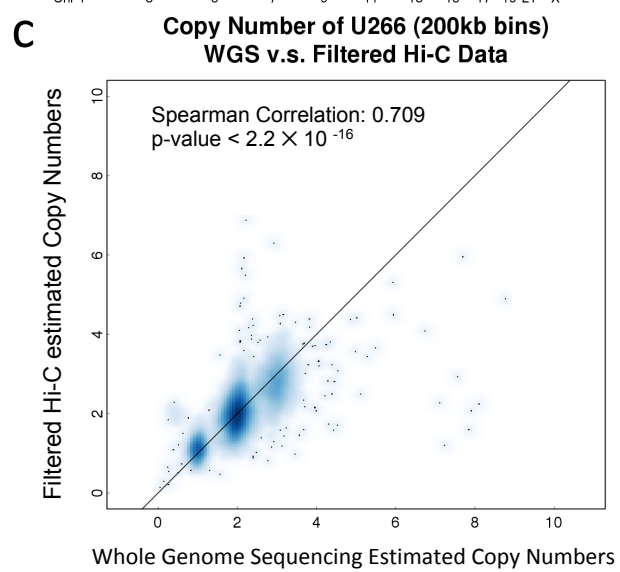
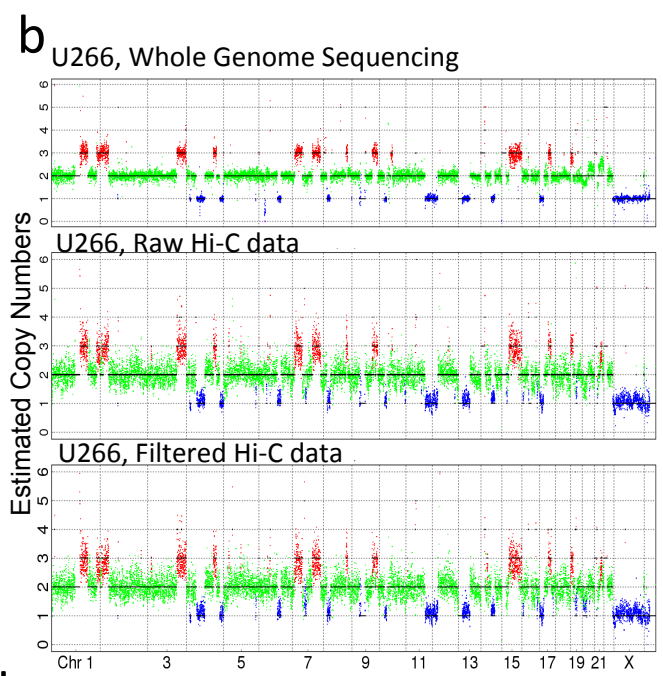
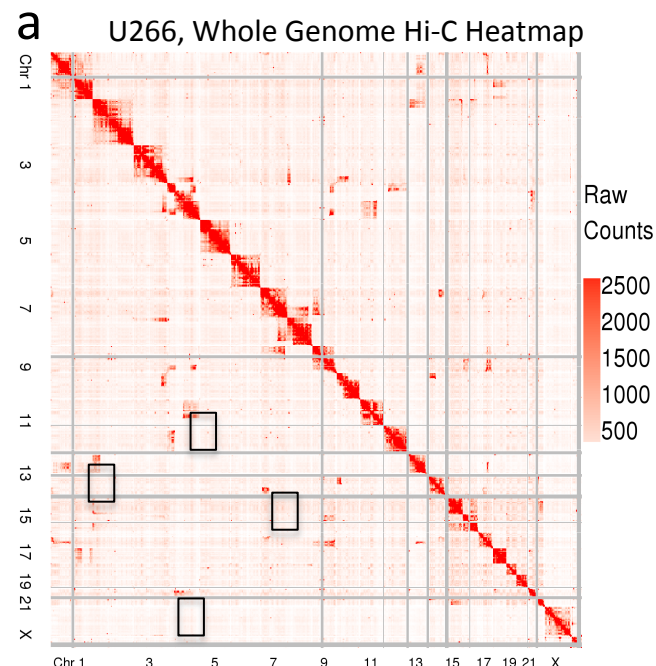


RPMI-8226, genome, Interactions

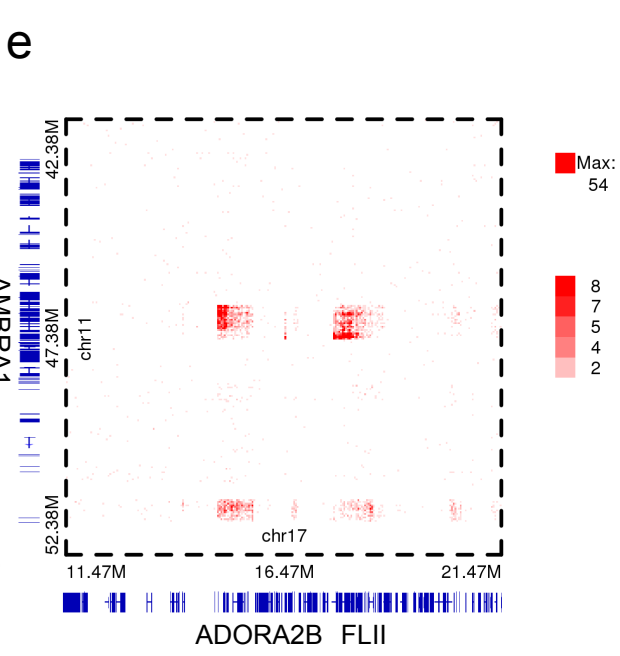
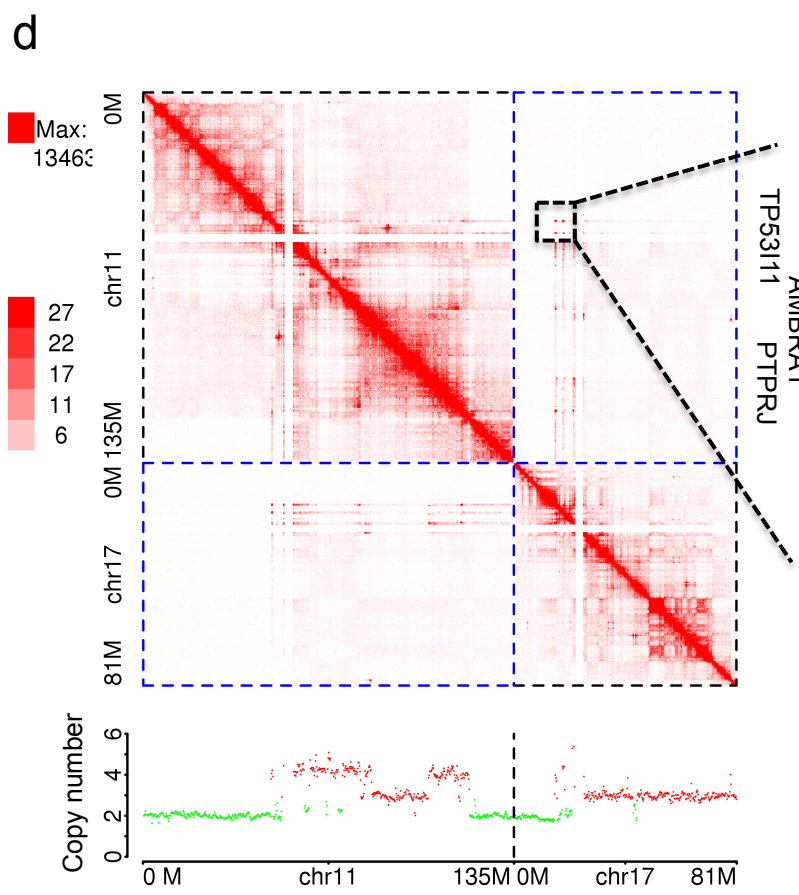
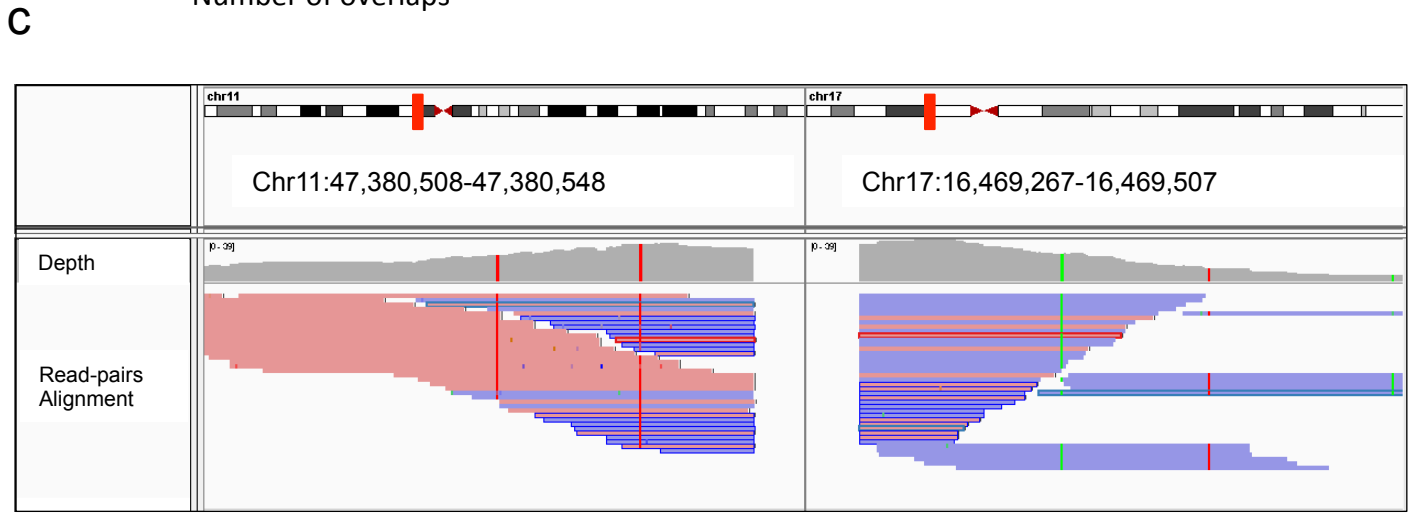
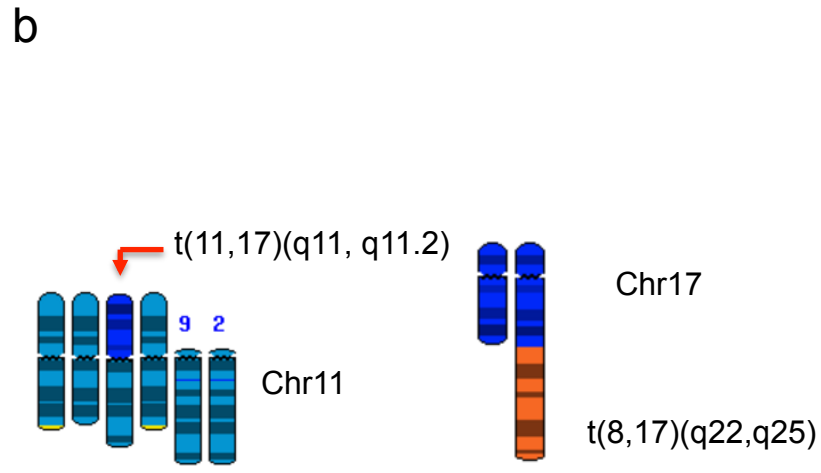
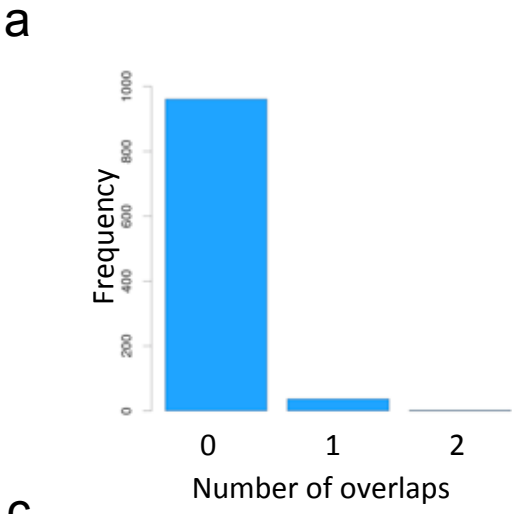


Supplementary Figure 2. Basic characterization of Hi-C, WGS and RNA-seq data.

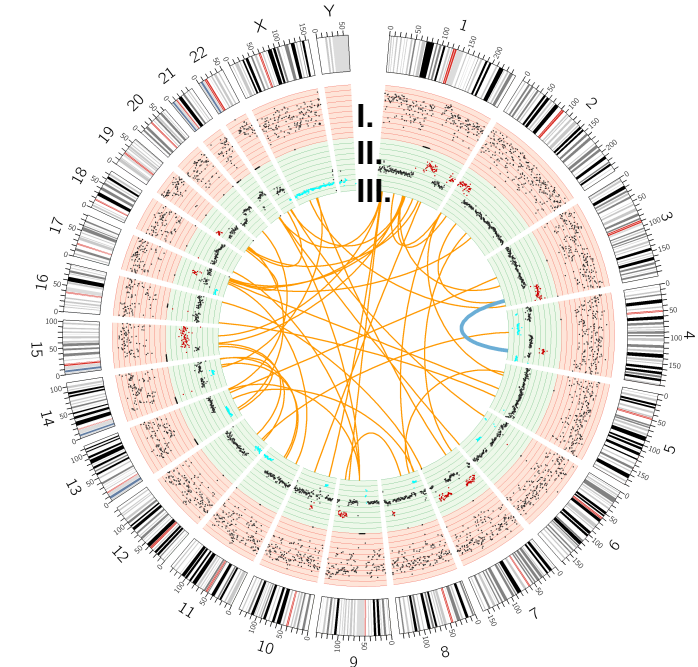
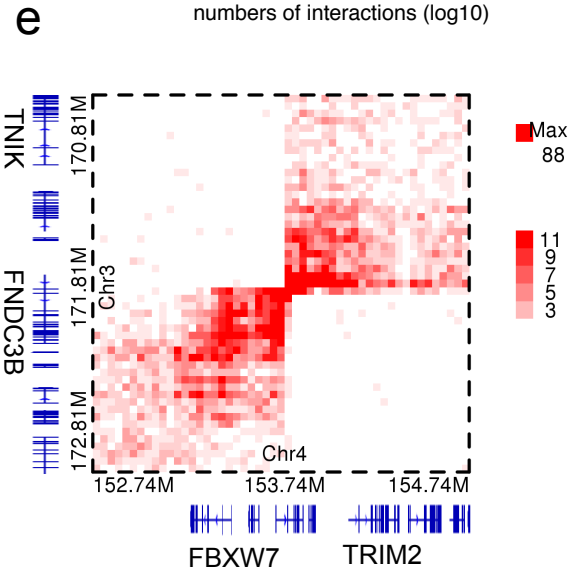
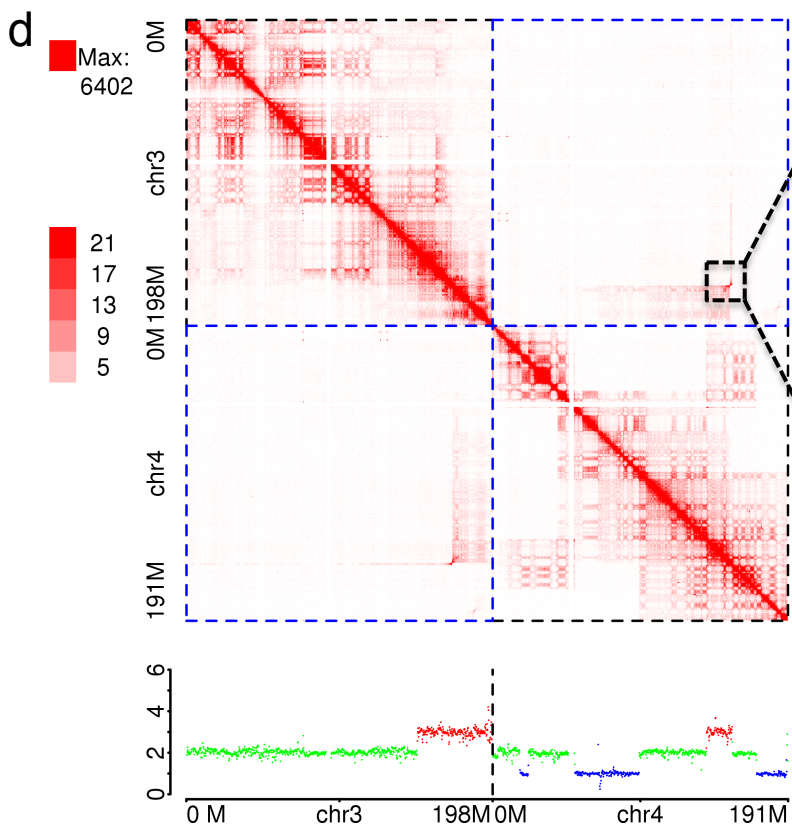
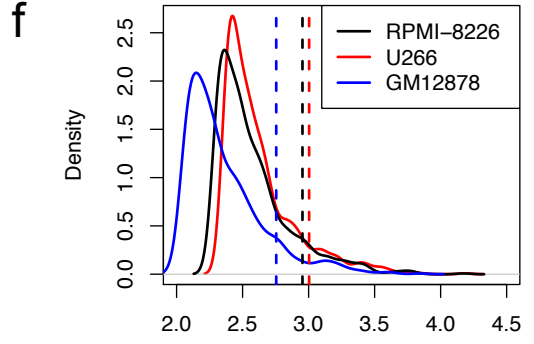
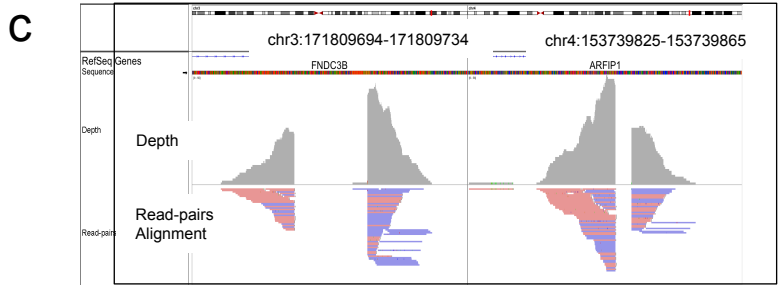
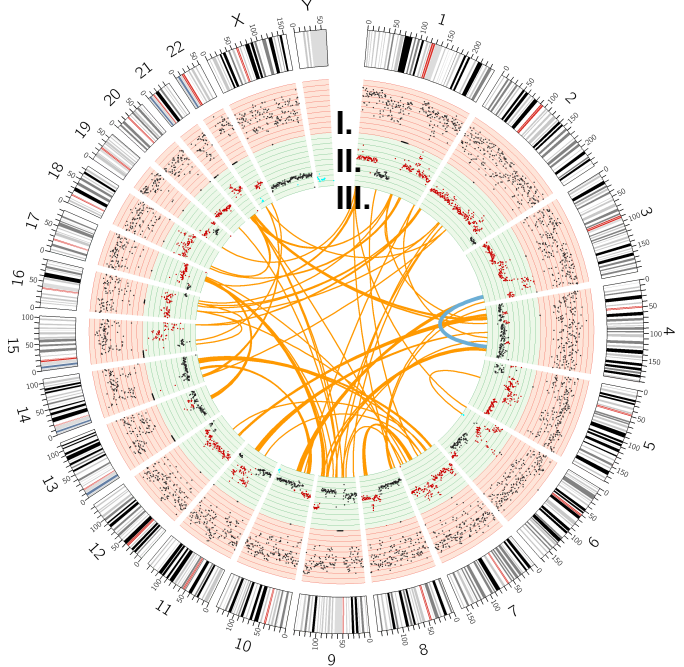
(a) Relative composition of different classes of Hi-C reads at different ranges of genomic spans. (b) Composition of paired-end Hi-C reads in different Hi-C experiments, as a function of the genomic distance between a pair of DNA fragments. (c) Contact matrix from the whole chromosome 1 at 200 kb resolution. Left: RPMI-8226 with HindIII, right: RPMI-8226 with Mbo I. (d) Left: Comparing interaction scores of chromosome 1 in RPMI-8226 (HindIII) at y-axis and RPMI-8226 (MboI) at x-axis, 200 kb resolution, the Pearson's r is 0.89; Right: Comparing interaction scores of whole genome in RPMI-8226 (HindIII) at y-axis and RPMI-8226 (MboI) at x-axis, at 3 M resolution, the Pearson's r is 0.87.



Supplementary Figure 3. Correcting copy number variation in cancer Hi-C data of U266 cells. See Figure 1 legend. The data are for U266 cells.



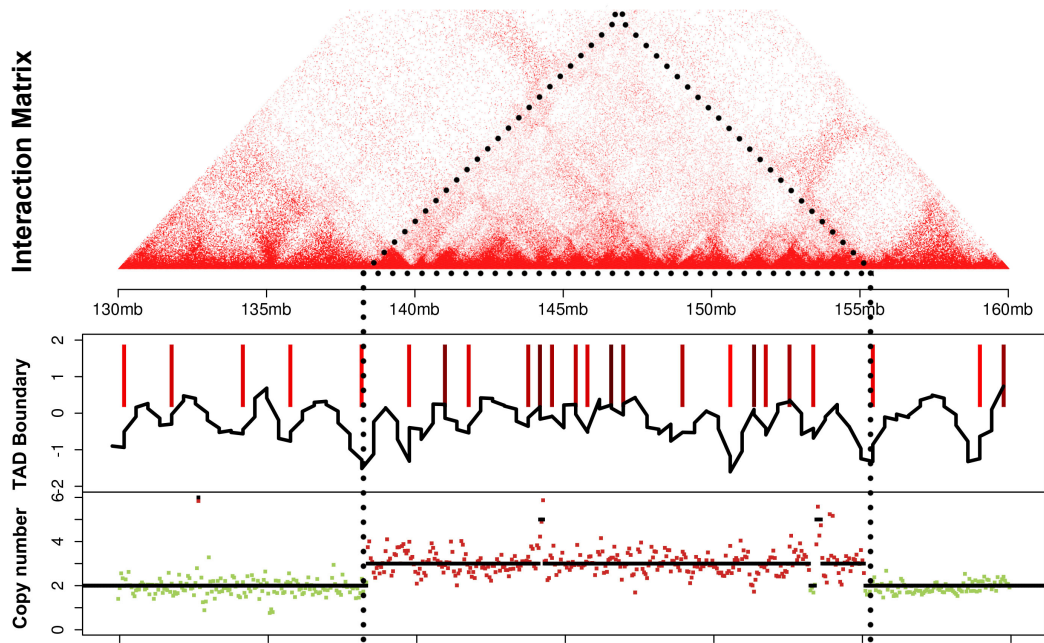
Supplementary Figure 4. In RPMI-8226, both Hi-C and WGS data identified the translocation of t(11,17)(q11, q11.2). (a) Overlap between random sites and translocation sites in RPMI 8226 cells. 100 random-sampled sites were used to calculate the overlap with WGS translocations for 1000 times. (b) The chimeric chromosome formed between chr11 and chr17 is identified by spectral karyotyping (SKY). The SKY image of RPMI-8226 is from the NCBI SKY database. (c) The translocation event of t(11;17)(q11;q11.2) in RPMI-8226 cells plotted by IGV tool, with only WGS paired reads supporting this translocation event. The reads depth and alignment panels are shown. Read alignments are sorted by read location and colored by read strands. (d) Hi-C interaction maps of chromosome 11 and 17 showed the translocation of t(11;17)(q11;q11.2) in RPMI-8226. Top panel: the intra and inter-chromosome interaction maps of chromosome 11 and 17 in RPMI-8226. Bottom panel: copy number variations of chromosome 11 and 17. (e) Enlarged inter-chromosomal interactions induced by the translocation event. Genes of ADOR2ZB, FLII, AMBRA1 and PTRPJ were affected by inter-chromosomal translocations. The AMBRA1 gene is a member of autophagy signaling network and recently been identified as a haploinsufficient tumor suppressor gene by regulating c-Myc¹. ADORA2B is a member of the G protein-coupled receptor superfamily and involved in the metastasis of breast cancer (PMC3612632).

a U266 Translocations**b** U266, Hi-C Top 100 Interaction Pairs

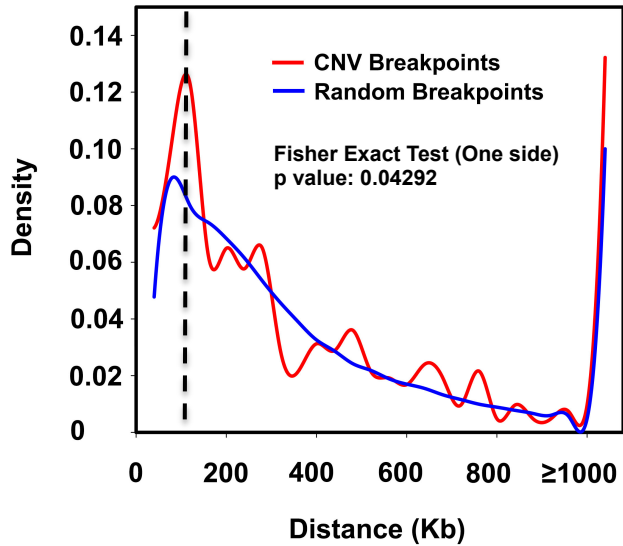
Supplementary Figure 5. In U266 cells, both Hi-C and WGS data identified the translocation between gene FNDC3B at 3q26.31 and gene FBXW7 at 4q33.2. (a)(b) See Figure 2 (a)(b) legends, The 42 inter-chromosome translocation events and top 100 highest inter-chromosome interactions, RNA-seq counts and copy numbers of U266 cells are used for circos plot . (c) The translocation event of t(3, 4)(q26.31, q31.3) in U266 cells plotted by IGV tool, with only WGS paired reads supporting this translocation event. The reads depth and alignment panels are shown. Read alignments are sorted by read location and colored by read strands. (d) Hi-C interaction maps of chromosome 3 and 4 showed the translocation of t(3, 4)(q26.31, q31.3) in U266. Top panel: the intra and inter-chromosome interaction maps of chromosome 3 and 4 in U266. Lower panel: the copy number variations of chromosome 3 and 4 in U266. (e) Enlarged inter-chromosomal interactions induced by the translocation event t(3, 4)(q26.31, q31.3) in U266. Genes of FNDC3B, FBXW7 and TRIM2 were affected by inter-chromosomal translocations. FNDC3B is a recently identified oncogene amplified in hepatocellular carcinoma and induces epithelial-to-mesenchymal transition ². FBXW7 is a ubiquitin ligase and tumor suppressor in many cancer types ³. In MM, FBXW7 is a pro-survival factor through degradation of p100 which target on NF-κB signaling ⁴. (f) Density plot for top 1000 inter-chromosomal interactions in three cell lines. Dash lines indicate 10% cutoff.

U266:chr4:130mb-160mb

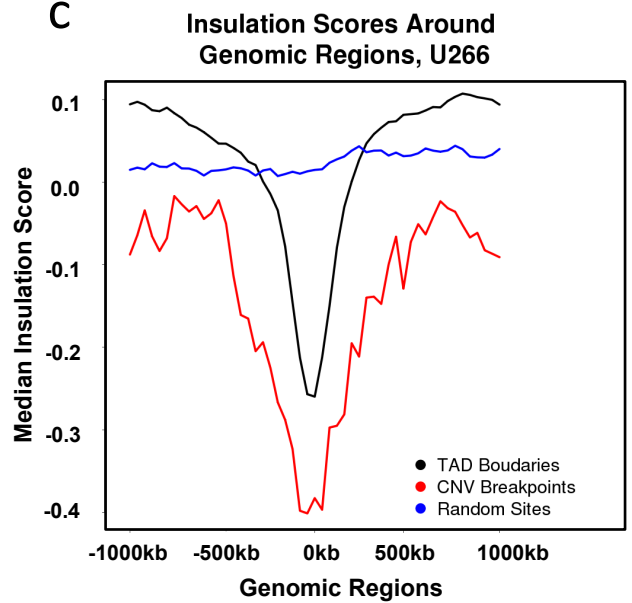
a



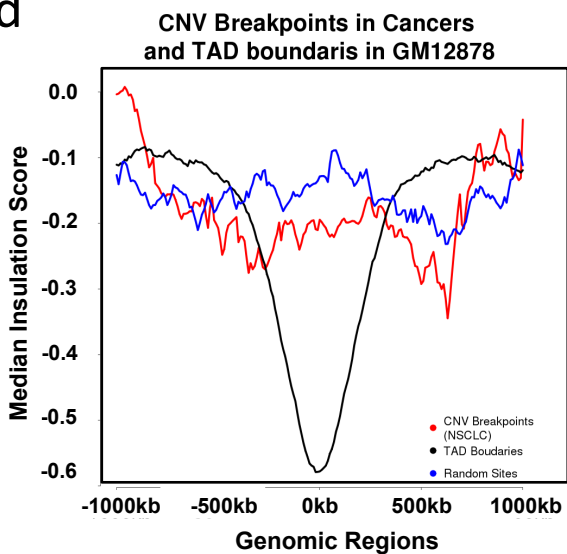
b



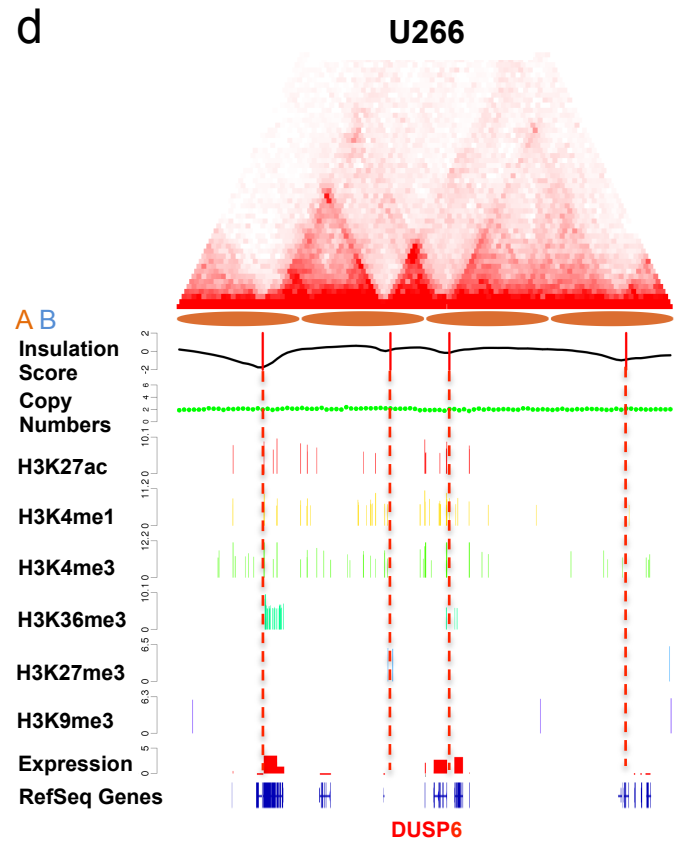
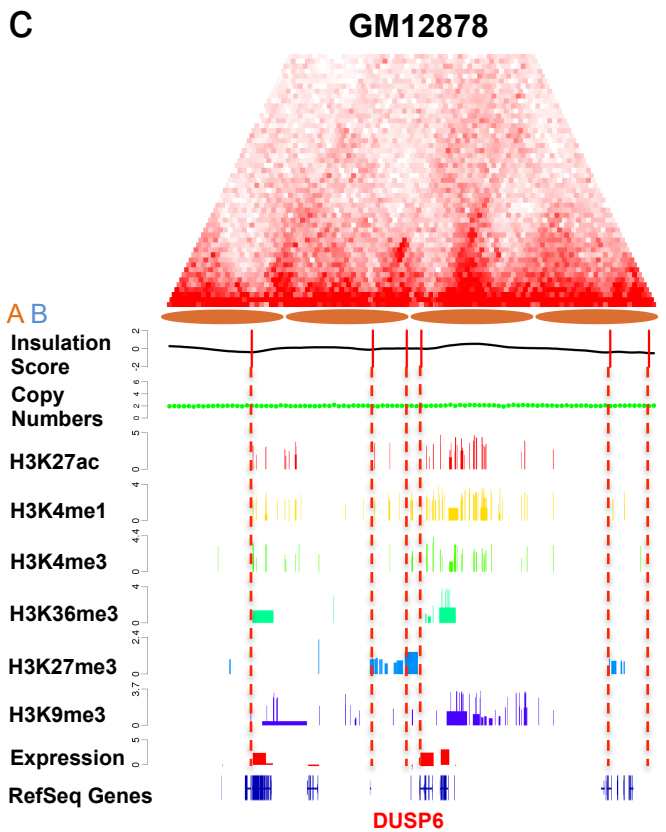
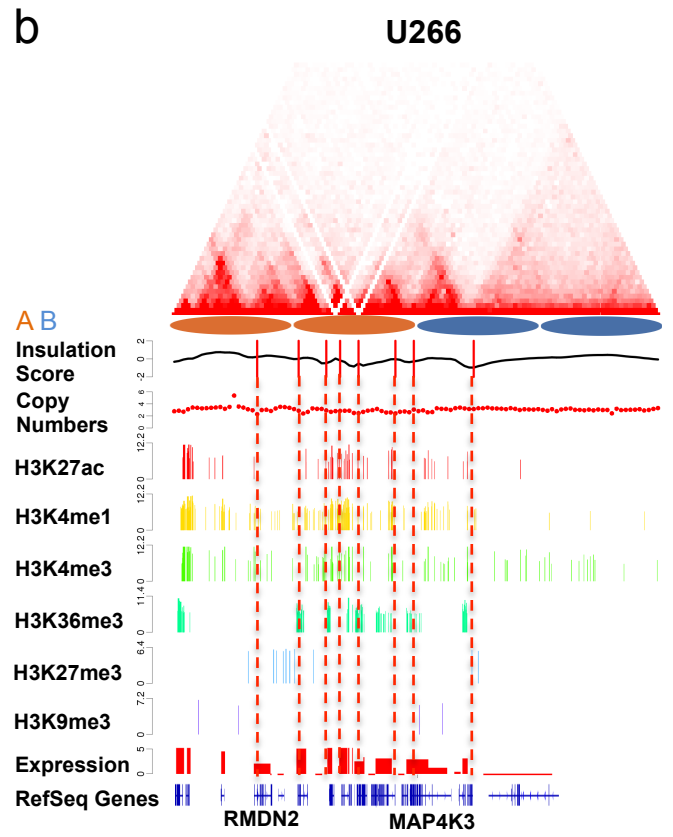
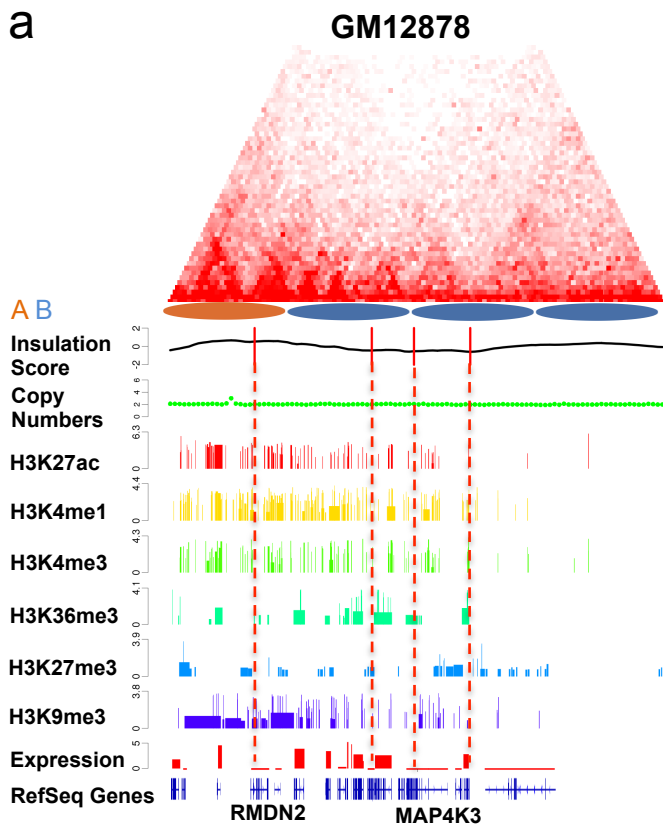
c



d



Supplementary Figure 6. CNV breakpoints associated with TAD boundaries in U266 cells. See Figure 3 legends. The data are for U266 cells.



Supplementary Figure 7. Example of MAPK pathway gene expression changes associated with spatial genome reorganization. (a) Expression and Hi-C heatmap of gene MAP4K3 in GM12878. (b) Expression and Hi-C heatmap of gene MAP4K3 in U266. Up-regulation of MAP4K3 is associated with both copy number gain and spatial genome reorganization. (c) Expression and Hi-C heatmap of gene DUSP6 in GM12878. (d) Expression and Hi-C heatmap of gene DUSP6 in U266. Up-regulation of DUSP6 is associated with spatial genome reorganization but not copy number variation.

Supplementary Table 1. Summary of sequencing data.

	Cell type	Enzyme	All reads	Filtered reads	Cis ratio
Hi-C	RPMI-8226	HindIII	217,829,046	92,668,774 (42.5%)	74.30%
	RPMI-8226	Mbol	122,227,090	81,041,306 (66.3%)	60.50%
	U266	HindIII	228,423,540	86,378,574 (37.8%)	77.10%
	U266	Mbol	207,191,357	131,383,082 (63.4%)	64.77%
DNA-seq (WGS)	RPMI-8226	-	619,194,153	-	-
	U266	-	646,773,193	-	-
RNA-seq	RPMI-8226	-	55,945,480 (3 repeats)	-	-
	U266	-	57,424,004 (3 repeats)	-	-

Supplementary References

1. Cianfanelli, V. *et al.* AMBRA1 links autophagy to cell proliferation and tumorigenesis by promoting c-Myc dephosphorylation and degradation. *Nat Cell Biol* **17**, 20-30 (2015).
2. Cai, C. *et al.* Activation of multiple cancer pathways and tumor maintenance function of the 3q amplified oncogene FNDC3B. *Cell cycle* **11**, 1773-1781 (2012).
3. Yumimoto, K. & Nakayama, K.I. Fbxw7 suppresses cancer metastasis by inhibiting niche formation. *Oncoimmunology* **4**, e1022308 (2015).
4. Busino, L. *et al.* Fbxw7 α - and GSK3-mediated degradation of p100 is a pro-survival mechanism in multiple myeloma. *Nature cell biology* **14**, 375-385 (2012).